Third International Conference on Inverse Design Concepts and Optimization in Engineering Sciences (ICIDES-III), Editor: G.S. Dulikravich, Washington D.C., October 23-25, 1991.

COMPARISON OF FOUR STABLE NUMERICAL METHODS FOR ABEL'S INTEGRAL EQUATION

Diego A. Murio and Carlos E. Mejía

Department of Mathematical Sciences
University of Cincinnati
Cincinnati, OH 45221-0025
U.S.A.

ABSTRACT

The 3-D image reconstruction from cone-beam projections in computerized tomography leads naturally, in the case of radial symmetry, to the study of Abel-type integral equations. If the experimental information is obtained from measured data, on a discrete set of points, special methods are needed in order to restore continuity with respect to the data. A new combined Regularized-Adjoint-Conjugate Gradient algorithm (introduced in this work), together with two different implementations of the Mollification Method (one based on a data filtering technique and the other on the mollification of the kernel function) and a regularization by truncation method (initially proposed for 2-D ray sample schemes and more recently extended to 3-D cone-beam image reconstruction) are extensively tested and compared for accuracy and numerical stability as functions of the level of noise in the data.

1. INTRODUCTION.

The difficult problem of determining the structure of an object from its 3-D cone-beam data projections is currently receiving considerable attention (see B. D. Smith, Ref [16]). When the object is known to be radially symmetric, its structure can be determined by using the inverse Abel transform. If the object does not have radial symmetry, it can be reconstructed, in principle, by using the inverse Radon transform.

Abel's integral equation can be written as

$$f(x) = \int_0^x g(s)\,(x - s)^{-1/2}\,ds, \quad 0 \le x \le 1, \tag{1}$$

where the function $f(x)$ is the data function and $g(s)$ is the unknown function. The exact solution is given by

$$g(x) = \frac{1}{\pi}\int_0^x f'(s)\,(x - s)^{-1/2}\,ds, \quad 0 \le x \le 1, \tag{2}$$

provided the derivative exists and $f(0) = 0$. (See R. Gorenflo and S. Vessella, Ref [6]).

It is well-known (References [1], [2], [4] and [6]) that Abel's integral equation is somewhat ill-posed, that is, small errors in the data $f(x)$ might cause large errors in the computed solution $g(x)$. Consequently, the direct use of formula (2) is very limited and special methods are needed.

Third International Conference on Inverse Design Concepts and Optimization in Engineering Sciences (ICIDES-III), Editor: G.S. Dulikravich, Washington D.C., October 23-25, 1991.

This paper has two main purposes. First, we present and briefly analyze a new stable method for the numerical solution of Abel's integral equation, Method I, by weakly coupling the original problem with its adjoint formulation obtaining a regularized system of linear equations which is then successfully solved by the conjugate gradient method. Second, we test and compare the numerical stability and the accuracy of Method I and three other known algorithms on several benchmark examples as a function of the amount of noise in the data.

Method II in this paper (see D. A. Murio, Ref [12]), is obtained by initially filtering the noisy data by discrete convolution with a suitable averaging kernel instead of mollifying the kernel function in equation (2), Method III, as required by K. Miller (Refs [10] and [11]) in his reconstruction algorithm for 2-D ray-sampling schemes. Method IV has been implemented by D. A. Murio, D. Hinestroza and C. E. Mejía (Ref [13]) based on a regularization by truncation technique initially proposed by B. K. P. Horn (Ref [9]) and recently extended to 3-D image reconstruction methods from cone-beam projections by B. D. Smith (Ref [15]).

In Section 2 we introduce the new Method I, analyze the consistency and stability properties of the algorithm and obtain an upper bound for the error. In Section 3, we describe the other procedures and discuss in detail the numerical implementation of all the methods involved. Section 4 is devoted to the numerical testing of the four algorithms and the presentation of several useful comparisons involving Methods I, II, III and IV. Some conclusions are included in Section 5.

2. REGULARIZED-ADJOINT-CONJUGATE GRADIENT METHOD. (Method I).

In a more abstract setting, equation (1) can be written as

$$Ag = f,$$

where A represents the Abel integral operator. For suitable functions h and q, the adjoint operator A^* is defined by

$$A^*h(x) = q(x) \equiv \int_x^1 h(s)\,(s-x)^{-1/2}\,ds, \qquad 0 \le x \le 1,$$

and it is clear that the homogeneous equation $A^*h = 0$ has the unique solution $h(x) \equiv 0$, $0 \le x \le 1$. Hence, as a direct consequence of Fredholm alternative (see P. R. Garabedian, Ref [5]), solving the singular equation $Ag = f$ for smooth but otherwise arbitrary data functions f satisfying $f(0) = 0$, is equivalent to solve the uncoupled system of linear integral equations

$$\begin{cases} Ag = f \\ A^* h = 0. \end{cases} \tag{3}$$

In order to help stabilize the inverse problem, we propose to solve, instead of (3), the weakly coupled system of equations

$$\begin{cases} Au - \alpha v = f \\ A^*v + \alpha u = 0, \qquad 0 < \alpha << 1, \end{cases} \tag{4}$$

by successive approximations. This system is equivalent to

Third International Conference on Inverse Design Concepts and Optimization in Engineering Sciences (ICIDES-III), Editor: G.S. Dulikravich, Washington D.C., October 23-25, 1991.

$$\begin{cases} Au - \alpha v = f \\ \alpha\beta A^* v + \alpha^2\beta u - u + u = 0, \end{cases}$$

where β is any nonzero real number to be determined. We elect β to depend on the iteration and rewrite the previous system as

$$\begin{cases} Au_n - \alpha v_n = f \\ \alpha\beta_n A^* v_n + \alpha^2\beta_n u_n - u_n + u_{n+1} = 0, \end{cases}$$

to obtain

$$\begin{cases} \alpha v_n = Au_n - f \\ u_{n+1} = u_n - \beta_n[\alpha^2 u_n + A^*(\alpha v_n)], \end{cases} \qquad n = 0,1,2,\ldots, \qquad (5)$$

u_0 arbitrary, usually 0.

Remarks:

1. Each iteration in (5) involves the solution of two "direct" problems: one corresponding to the original operator, Au_n, and the other associated with the adjoint operator, $A^*(\alpha v_n)$.

2. Elimination of v in system (4) leads to the set of normal equations, with I indicating the identity operator,

$$(A^*A + \alpha^2 I)u = A^* f, \qquad (6)$$

which characterizes the minimum of the zero order Tikhonov functional (see C. W. Groetsch, Ref [7])

$$J(u) = \frac{1}{2}\left(\| Au - f \|^2 + \alpha^2 \| u \|^2 \right). \qquad (7)$$

3. The gradient of the functional (7) is given by

$$\nabla J(u) = \alpha^2 u + A^*(Au - f)$$

and it is easily computed if the solution of the adjoint problem is known. In fact, taking into consideration (4), we can write $\nabla J(u) = \alpha^2 u + A^*(\alpha v)$, and for each iteration we get

$$\nabla J(u_n) = \alpha^2 u_n + A^*(\alpha v_n). \qquad (8)$$

These considerations allow us to choose β_n, for each n, in such a manner that system (5) can now be solved by the Conjugate Gradient Method (W. M. Patterson, Ref [14]).

The complete abstract algorithm, after introducing the notations $(f,g) \equiv \int_0^1 f(x)g(x)\,dx$ and $\| f \| \equiv (f,f)^{1/2}$, corresponding to the inner product and

Third International Conference on Inverse Design Concepts and Optimization in Engineering Sciences (ICIDES-III), Editor: G.S. Dulikravich, Washington D.C., October 23-25, 1991.

norm respectively of square integrable functions on the interval [0,1], is as follows:

For n = 0,

0) Set $u_0 = 0$ and choose $\alpha > 0$.

1) Compute Au_0, i.e., solve the original direct problem.

2) Compute the residual $\alpha v_0 = Au_0 - f$.

3) Compute $A^*(\alpha v_0)$, i.e., solve the direct adjoint problem.

4) Evaluate the gradient $d_0 = \nabla J(u_0)$ using formula (8).

5) Set $r_0 = \dfrac{\| d_0 \|^2}{\alpha^2 \| d_0 \|^2 + \| Ad_0 \|^2}$.

6) Update: $u_1 = u_0 - r_0 d_0$.

For n = 1,2,...,

1') Solve the original direct problem Au_n.

2') Compute the residual $\alpha v_n = Au_n - f$.

3') Solve the direct adjoint problem $A^*(\alpha v_n)$.

4') Evaluate the gradient $\nabla J(u_n)$ using formula (8).

4'') Compute $d_n = \nabla J(u_n) + \dfrac{\| \nabla J(u_n) \|^2}{\| \nabla J(u_{n-1}) \|^2} d_{n-1}$.

5') Set $r_n = \dfrac{(\nabla J(u_n), d_n)}{\alpha^2 \| d_n \|^2 + \| Ad_n \|^2}$.

6') Update: $u_{n+1} = u_n - r_n d_n$.

Stability of Method I.

We consider now the more realistic situation when instead of the exact data function f, we only know some noisy data function f^ε satisfying

$$\| f - f^\varepsilon \| \leq \varepsilon.$$

In this section the unique solution of system (4) will be denoted by u_α^ε to emphasize its dependency on the regularization parameter α and the level of noise in the data ε. Assuming that the ideal problem (1) for errorless data f has the unique solution $g = A^{-1}f$, since u_α^ε satisfies equation (6), with f replaced by f^ε, it follows from well-known estimates in the theory of Tikhonov regularization that

$$\| g - u_\alpha \| = C_0 \alpha^{1/2}, \quad \text{and} \quad \| u_\alpha - u_\alpha^\varepsilon \| \leq \varepsilon \alpha^{-1/2},$$

for some constant $C_0 > 0$, independent of α; u_α denotes the regularized solution when $\varepsilon = 0$.

Combining these estimates, we obtain the error upper bound

Third International Conference on Inverse Design Concepts and Optimization in Engineering Sciences (ICIDES-III), Editor: G.S. Dulikravich, Washington D.C., October 23-25, 1991.

$$|| g - u_\alpha^\varepsilon || \le C_0 \alpha^{1/2} + \varepsilon \alpha^{-1/2}$$

and choosing $\alpha = C_1\varepsilon$ for some constant $C_1 > 0$, it follows that

$$|| g - u_\alpha^\varepsilon || \le (C_0 + C_1^{-1}) \alpha^{1/2} \tag{9}$$

which shows that, theoretically, as the quality of the data becomes better and better ($\varepsilon \to 0$), we get convergence with rate $\alpha^{1/2}$. See C. W. Groetsch (Ref [7]) for details.

The convergence of the sequence of iterates $u_{\alpha,n}^\varepsilon$ from system (5), with β_n as discussed above, to the unique solution u_α^ε of the canonical equations (6) as $n \to \infty$ is well documented, for instance, in the work of C. W. Groetsch, J. T. King and D. A. Murio (Ref [8]) and will not be pursued further here.

The finite dimensional version of the combined Regularized-Adjoint-Conjugate Gradient algorithm will be discussed in the next Section.

3. METHODS II, III AND IV. NUMERICAL IMPLEMENTATIONS.

Method II in this paper is based on attempting to reconstruct a mollified version of the solution g in equation (2). After introducing the δ-mollifier

$$p_\delta(x) = \frac{1}{\delta} \pi^{-1/2} \exp[-x^2/\delta^2] \tag{10}$$

of "blurring radius" δ and extending the data function f^ε to the interval $[-3\delta,1+3\delta]$ in such a way that it decays smoothly to zero on $[1,1+3\delta]$ and it is zero on $[-3\delta,0]$, an approximate solution is defined by

$$g_\delta^\varepsilon(x) = \frac{1}{\pi} \int_0^x (p_\delta * f^\varepsilon)'(s) \, (x - s)^{-1/2} \, ds, \qquad 0 \le x \le 1. \tag{11}$$

Here,

$$(p_\delta * f^\varepsilon)'(x) = \int_{-\infty}^{\infty} \frac{d}{dx} [p_\delta(x - s) \, f^\varepsilon(s)] \, ds \approx \int_{x-3\delta}^{x+3\delta} \frac{d}{dx} [p_\delta(x - s) \, f^\varepsilon(s)] \, ds,$$

showing that the main idea of the method consists on replacing the noisy data function f^ε by the filtered data function $p_\delta * f^\varepsilon$. It is important to notice that the radius of mollification, δ, can be uniquely and automatically determined as a function of the amount of noise in the data, ε, based in the fact that there is a unique value of the regularizing parameter δ for which

$$|| p_\delta * f^\varepsilon - f^\varepsilon || = \varepsilon. \tag{12}$$

Under very mild conditions, i.e., if f^ε is continuous and if the second derivative of the errorless data function f is uniformly bounded by M_2 in the

Third International Conference on Inverse Design Concepts and Optimization in Engineering Sciences (ICIDES-III), Editor: G.S. Dulikravich, Washington D.C., October 23-25, 1991.

sample interval (0,1), the following error estimate holds

$$\| g_\delta^\varepsilon - g \| \le \frac{6}{\pi} (\delta M_2 + \varepsilon/\delta). \tag{13}$$

The complete abstract algorithm is as follows:

1) Automatically determine the unique radius of mollification δ as a function of the level of noise ε.

2) Smoothly extend the noisy data function f^ε to $[-3\delta,1+3\delta]$.

3) Compute the derivative of the filtered data function $p_\delta * f^\varepsilon$.

4) Compute g_δ^ε using equation (11).

For more details and further discussions, the reader should consult D. A. Murio, Ref [12].

Method III is based on the Mollification Method as originally proposed by K. Miller (Refs [10] and [11]) for 2-D ray-sampling reconstruction geometries. First we notice that the exact formula (2) can be written

$$g(x) = \frac{1}{\pi} (k * f')(x), \qquad 0 \le x \le 1,$$

where $k(t) = t^{-1/2}$ represents the kernel function. The mollification of the last equation with the averaging kernel defined in (10) gives

$$(p_\delta * g)(x) = \frac{1}{\pi} (p_\delta * k * f')(x).$$

In Method II, we associated the right-hand side of this equation as $k * (p_\delta * f') = k * (p_\delta * f)'$; for Miller's idea we associate as $(p_\delta * k) * f' = (p_\delta * k)' * f$ and obtain the approximate reconstruction solution

$$g_\delta^\varepsilon(x) = \frac{1}{\pi} \int_0^x (p_\delta * k)'(x - s)\, f^\varepsilon(s)\, ds, \qquad 0 \le x \le 1. \tag{14}$$

Mathematically, formulae (11), for Method II, and (14), for Method III, are identical. Consequently, the theoretical error bound (13) derived for Method II also applies for Method III.

The complete abstract algorithm for Method III is given by:

1) Choose $\delta > 0$.

2) Compute the mollified kernel $p_\delta * k$.

3) Evaluate the derivative of the mollified kernel $p_\delta * k$.

4) Compute g_δ^ε using equation (14).

Remarks:

1. In Method III, the mollified kernel is computed only once and is used repeatedly for different data functions.

Third International Conference on Inverse Design Concepts and Optimization in Engineering Sciences (ICIDES-III), Editor: G.S. Dulikravich, Washington D.C., October 23-25, 1991.

2. Method II requires a filtering of each data function and the corresponding parameter is automatically selected according to the quality of the measured data.
3. The selection of the mollification parameter in Method III requires further consideration.

Method IV is based on a reconstruction technique initially proposed by B. K. P. Horn (Ref [9]) for arbitrary 2-D ray schemes and more recently extended to 3-D image reconstruction methods from cone-beam projections by B. D. Smith (Ref [15]).

Integrating by parts equation (2), we obtain the equivalent expression

$$g(x) = \frac{1}{\pi} \lim_{\gamma \to 0} \left\{ \gamma^{-3/2} \int_{x-\gamma}^{x} f(s)\, ds - \frac{1}{2} \int_{0}^{x-\gamma} f(s)(x-s)^{-3/2} ds \right\}, \qquad 0 \le x \le 1.$$

The approximate inverse Abel transform is now obtained by eliminating the limit procedure in the last expression, i.e.,

$$g_\gamma^\varepsilon(x) = \frac{1}{\pi} \left\{ \gamma^{-3/2} \int_{x-\gamma}^{x} f^\varepsilon(s)\, ds - \frac{1}{2} \int_{0}^{x-\gamma} f^\varepsilon(s)\, (x - s)^{-3/2}\, ds \right\}, \qquad 0 \le x \le 1. \quad (15)$$

By requiring the second derivative of the errorless data function f and the measured data function f^ε to be continuous, we obtain the following error estimate

$$\| g_\gamma^\varepsilon - g \| \le \frac{5}{2} \frac{\gamma^{1/2}}{\pi} M_1 + \frac{2}{\pi} \varepsilon\, \gamma^{-1/2} + O(\gamma^{3/2}), \quad (16)$$

where M_1 is a uniform bound for f' on the interval (0,1). For a proof of this assertion and a complete analysis of Method IV, see D. A. Murio, D. Hinestroza and C. E. Mejía (Ref [13]).

The complete abstract algorithm for Method IV is reduced to

1) Choose $\gamma > 0$.
2) Compute g_γ^ε using formula (15).

Remark:

The error estimates (9), (13) and (16) show that all the methods are consistent and stable with respect to perturbations in the data, in the L_2 norm, for a fixed choice of the several regularization parameters α, δ or γ.

Numerical Implementations.

Since in practice only a discrete set of data points is generally available, we assume that the data function f^ε is a discrete function measured at equally spaced sample points on the interval [0,1]. For $h > 0$ and $Nh = 1$, we let $x_j = jh$ and denote $f^\varepsilon(x_j) = f_j^\varepsilon$, $j = 0,1,\ldots,N$, with $f_0^\varepsilon = 0$.

Method I:

Discretization leads to a finite dimensional version of the combined Regularized-Adjoint-Conjugate Gradient algorithm of Section 2. The operators A and A^* are represented now by a matrix A and its transpose A^T, respectively. The

Third International Conference on Inverse Design Concepts and Optimization in Engineering Sciences (ICIDES-III), Editor: G.S. Dulikravich, Washington D.C., October 23-25, 1991.

approximate discrete solution $u^{\varepsilon}_{m,\alpha}$, obtained after m iterations, the gradient $\nabla J(u_m)$, d_m, r_m, u_0 and the residual αv_m are now N-dimensional real vectors. From equation (1), a simple discretization gives the lower triangular system of linear equations

$$h \sum_{i=1}^{j} a_{j+1-i}(u^{\varepsilon}_{m,\alpha})_i = f^{\varepsilon}_j ,$$

where

$$a_j = (jh)^{-1/2}, \qquad j = 1,2,\ldots,N,$$

indicates the (j-1) subdiagonal of the N x N matrix A.

The discrete algorithm for the Conjugate Gradient method (see P. G. Ciarlet, Ref [3]) follows exactly the steps described previously in Section 2, and we only have to add the necessary stopping criteria, given by

$$\| u^{\varepsilon}_{m,\alpha} - u^{\varepsilon}_{m-1,\alpha} \|_2 \le TOL \, \| u^{\varepsilon}_{m,\alpha} \|_2,$$

where TOL is a small positive tolerance parameter entered by the user and

$$\| f \|_2 = \left\{ \frac{1}{N} \sum_{j=0}^{N} [f_j]^2 \right\}^{1/2} \tag{17}$$

is the discrete l_2 norm on [0,1].

Method II:

To numerically approximate $g^{\varepsilon}_{\delta}(x)$, a quadrature formula for the convolution equation (11) is required. The objective is to introduce a simple approximation and avoid any artificial smoothing in the process.

Given x_j, j = 0,1,...,N, we define

$$q^{\varepsilon}(x) = \sum_{i=0}^{j} f^{\varepsilon}_i \phi_i(x), \qquad 0 \le x \le x_j,$$

a piecewise constant interpolation of $f^{\varepsilon}(x)$ at the grid points x_j. Here,

$$\phi_0(x) = \begin{cases} 1, & 0 \le x \le h/2 \\ 0, & \text{otherwise} \end{cases}, \qquad \phi_j(x) = \begin{cases} 1, & x_j - h/2 \le x \le x_j \\ 0, & \text{otherwise} \end{cases}$$

and

$$\phi_i(x) = \begin{cases} 1, & x_i - h/2 \le x \le x_i + h/2 \\ 0, & \text{otherwise} \end{cases}, \quad i = 1,2,\ldots,j-1.$$

The computational algorithm is as follows:

After smoothly extending the discrete data function to any interval of interest containing the sample interval [0,1], we determine the radius of mollification δ as

Third International Conference on Inverse Design Concepts and Optimization in Engineering Sciences (ICIDES-III), Editor: G.S. Dulikravich, Washington D.C., October 23-25, 1991.

a function of the amount of noise in the data ε by solving the discrete version of equation (12) using the bisection method. Next, we substitute f^ε by its interpolation q^ε and compute the approximation to $p_\delta * f^\varepsilon$ given by the discrete convolution

$$(p_\delta * q^\varepsilon)(x) = \sum_k f_k^\varepsilon (p_\delta * \phi_k)(x_j) = \sum_k f_k^\varepsilon \, m_j^\delta,$$

where the weights m_j^δ are evaluated exactly. A discrete version of the derivative of the discrete filtered data function is obtained using centered finite differences. Finally, the discrete approximation to g_δ^ε is calculated by discretely convolving the computed derivative approximation against the sampled data function (see equation (11)). For a detailed analysis of this algorithm, the reader is referred to D. A. Murio (Ref [12]).

Method III:

The convolution $p_\delta * k$ requires an extension of the singular kernel k for values of x less or equal to zero. In our implementation we use the following symmetric extension:

$$k(0) = 2h^{-1/2}, \quad k(-x) = k(x), \quad x > 0.$$

The discrete approximation is now straightforward:
With $s_j = (p_\delta * k)(x_j)$, $j = 0,1,\ldots,N$, the discrete convolution formula corresponding to equation (14) is

$$g_{h,\delta}^\varepsilon(0) = 0,$$

$$g_{h,\delta}^\varepsilon(x_j) = \frac{1}{\pi} \sum_{k=1}^{j} s_{j-k}(f_{k+1}^\varepsilon - f_{k-1}^\varepsilon)/2, \qquad j = 1,2,..,N-1$$

and

$$g_{h,\delta}^\varepsilon(1) = g_{h,\delta}^\varepsilon(x_{N-1}) + \frac{1}{\pi} s_0(f_N^\varepsilon - f_{N-1}^\varepsilon),$$

where $g_{h,\delta}^\varepsilon$ is the approximate inverse Abel transform at the grid points.

Method IV:

In this case, we first construct a piecewise linear interpolation of $f^\varepsilon(x)$ at the grid points x_j, given by

$$q^\varepsilon(x) = \sum_{i=0}^{j} f_j^\varepsilon \, \phi_i(x), \qquad 0 \le x \le x_j,$$

where the functions $\phi_i(x)$, $i = 0,1,\ldots,N$ are given by

Third International Conference on Inverse Design Concepts and Optimization in Engineering Sciences (ICIDES-III), Editor: G.S. Dulikravich, Washington D.C., October 23-25, 1991.

$$\phi_0(x) = \begin{cases} 1-x/h, & 0 \le x \le h \\ 0 & \text{otherwise,} \end{cases} \qquad \phi_j(x) = \begin{cases} 1+(x-x_j)/h, & x_{j-1} \le x \le x_j \\ 0 & \text{otherwise,} \end{cases}$$

and

$$\phi_i(x) = \begin{cases} 1+(x-x_i)/h, & x_{i-1} \le x \le x_i \\ 1-(x-x_i)/h, & x_i \le x \le x_{i+1} \\ 0 \text{ otherwise,} \end{cases} \qquad i = 1,2,\ldots,j.$$

We notice that the approximate solution $g_\gamma^\varepsilon(x)$ of formula (15) can also be written as

$$g_\gamma^\varepsilon(x) = \frac{1}{\pi} (H_\gamma * f^\varepsilon)(x), \quad 0 \le x \le 1, \tag{18}$$

where the kernel H_γ is defined by

$$H_\gamma(t) = \begin{cases} \gamma^{-3/2}, & 0 \le t < \gamma \\ -\frac{1}{2} t^{-3/2}, & \gamma \le t. \end{cases}$$

The quadrature formula for equation (18) is obtained by directly convolving the kernel function H_γ with q^ε as indicated below. Thus, the computed solution at the grid points is given by

$$g_{\gamma,h}^\varepsilon(x_j) = \frac{1}{\pi} (H_\gamma * q^\varepsilon)(x_j) = \frac{1}{\pi} \sum_{i=0}^{j} f_i^\varepsilon \, b_i^\gamma(x_j),$$

where the weights

$$b_i^\gamma(x_j) = \int_0^{x_j} H_\gamma(x_j - s) \, \phi_i(s) \, ds$$

are evaluated exactly for $i = 0,1,\ldots,j$. The readers interested in further details should consult D. A. Murio, D. Hinestroza and C. E. Mejía (Ref [13]).

4. NUMERICAL RESULTS AND COMPARISON.

In this section we describe the tests that have been implemented in order to compare the performance of the methods introduced in previous sections.

We tested the methods on three examples. In all of them, the exact data function is denoted $f(x)$ and the noisy data function $f^\varepsilon(x)$ is obtained by adding an ε random error to $f(x)$, that is, $f^\varepsilon(x_j) = f(x_j) + \varepsilon\sigma_j$, where $x_j = jh$, $j = 0,1,\ldots,N$; $Nh = 1$ and σ_j is a uniform random variable with values in $[-1,1]$ such that

$$\max_{0 \le j \le N} | f^\varepsilon(x_j) - f(x_j) | \le \varepsilon.$$

The exact inverse Abel transform is denoted $g(x)$ and its approximation given by

Third International Conference on Inverse Design Concepts and Optimization in Engineering Sciences (ICIDES-III), Editor: G.S. Dulikravich, Washington D.C., October 23-25, 1991.

any of the methods is denoted $g^{\varepsilon}_{p,h}(x)$, where p represents the regularization parameter of the particular method.

Example 1:

As a first example we consider the data function $f(x) = x$ with exact inverse Abel transform $g(x) = \frac{2}{\pi} x^{1/2}$. This data function satisfies all the necessary hypotheses for convergence estimates of Sections 2 and 3.

Example 2:

The data function

$$f(x) = \begin{cases} 2x^2, & 0 \le x < 1/2 \\ 1-2(1-x)^2, & 1/2 \le x \le 1, \end{cases}$$

is only once continuously differentiable on [0,1], partially violating the required conditions for the theoretical error analysis of Sections 2 and 3. In this example, the exact inverse Abel transform is given by

$$g(x) = \begin{cases} (16/3\pi)x^{3/2}, & 0 \le x \ 1/2 \\ (16/3\pi)x^{3/2} + (16/3\pi)(x-1/2)^{3/2} - (8/\pi)(x-1/2)^{1/2}(2x-1), \\ \qquad 1/2 < x \le 1. \end{cases}$$

Example 3:

The data function is defined as follows:

$$f(x) = \begin{cases} 0, & 0 \le x < 0.2, \\ 2(x-0.2)^{1/2}, & 0.2 \le x \le 0.6, \\ 2(x-0.2)^{1/2} - 2(x-0.6)^{1/2} & 0.6 < x \le 1. \end{cases}$$

Its first derivative is not continuous on [0,1], strongly violating the necessary hypotheses for the convergence estimates of Sections 2 and 3. The exact inverse Abel transform is given by

$$g(x) = \begin{cases} 1, & 0.2 \le x \le 0.6, \\ 0, & \text{otherwise.} \end{cases}$$

The four methods were tested for three different values of N, N = 200, 500 and 1000, three different values of ε, ε = 0.0, 0.005 and 0.01, and several values of the corresponding regularization parameters. The algorithms were extensively used and we numerically determined appropriate values for the regularization parameters for each method, except for Method II where the radius of mollification was selected automatically. These quasi-optimal parameter values are used in the tables and figures below.

Third International Conference on Inverse Design Concepts and Optimization in Engineering Sciences (ICIDES-III). Editor: G.S. Dulikravich, Washington D.C., October 23-25, 1991.

Different values of ε provide a crucial test for stability. Tables 1, 2 and 3 illustrate this point. The error norms in the tables are computed as $\| g - g^{\varepsilon}_{p,h} \|_2$ according to definition (17). In the tables, each row corresponds to one of the methods with a fixed regularization parameter, and shows the change in the error norm due to changes in the level of noise in the data. The presented numerical results indicate stability. The columns in the tables allow us to compare the performance of the methods under similar conditions.

Figures 1 to 4 show the reconstructions of the step function of Example 3 provided by the four methods for the same number of sample data points, N = 500, the same noise level, ε = 0.01, and quasi-optimal regularization parameters. The qualitative behavior is quite good taken into consideration the high amount of noise in the data.

5. CONCLUSIONS

The following are some conclusions based on the implementations of the methods presented in this paper:

Consistency and stability of the four methods is clearly confirmed throughout experimentation and very weak dependency on the parameter N is observed.

Method II provides an automatic mechanism to select the radius of mollification as a function of the level of noise in the data. Furthermore, as a consequence of the stability of the four methods, it is easy to find, by numerical experimentation,lower and upper bounds for quasi-optimal regularization parameters.

An advantage of method III over method II is that the mollification of the kernel is computed only once and can be used for different data functions. Methods II applies mollification to each data set.

All the results are very competitive. However, mollification solutions are slightly better in terms of accuracy and method IV, the easiest to implement, seems to be more sensitive to perturbations in the data.

REFERENCES

1. Baker, C.T.H., The Numerical Treatment of Integral Equations, Clarendon Press, Oxford, 1977.

2. Baker, C.T.H., An Introduction to the numerical treatment of Volterra and Abel-type integral equations. Lecture Notes in Mathematics 965, Springer-Verlag, 1982, 1-38.

3. Ciarlet, P.G,, Introduction to Numerical Linear Algebra and Optimisation, Cambridge University Press, Cambridge, 1989.

4. Delves, L.M. and J. Walsh, editors. Numerical solution of Integral Equations, Clarendon Press, Oxford, 1974.

5. Garabedian, P. R., Partial Differential Equations, John Wiley and Sons, New York, 1964.

6. Gorenflo, R. and S. Vessella, Abel Integral Equations; Analysis and Applications, Lecture Notes in Mathematics 1461, Springer-Verlag, 1991.

7. Groetsch, C. W., The theory of Tikhonov regularization for Fredholm equations of the first kind, Pitman, 1984.

8. Groetsch, C. W., J. T. King and D. A. Murio, Asymptotic Analysis of a Finite Element Method for Fredholm equations of the first kind, in Treatment of Integral Equations by Numerical Methods. C. T. H. Baker and G. F. Miller, editors. Academic Press, 1982, 1-11.

9. Horn, B. K. P., Density reconstruction using arbitrary ray-sampling schemes, Proc. IEEE, Vol. 66, No. 5, 1978, pp. 551-562.

10. Miller, K., An optimal method for the x-ray reconstruction problem, preliminary report, Amer. Math. Soc. Notices, January, 1978, A-161.

11. Miller, K., New results on reconstruction methods from x-ray projections, Lecture Notes (unpublished), Department of Mathematics, University of Firenze, December, 1978, available from the author.

12. Murio, D. A., Stable numerical inversion of Abel's integral equation by discrete mollification, to appear in SIAM Proceedings on Design Theory, Great Lakes Section, Wright-Patterson Air Force Base, Dayton, Ohio, April 1990.

13. Murio, D. A., Hinestroza, D. and Mejía, C. E., New stable numerical inversion of Abel's integral equation, to appear in Proceedings Third International Symposium of Numerical Analysis, Madrid, Spain, May 1990.

14. Patterson, W. M., Iterative Methods for the Solution of Linear Operator Equations in Hilbert Spaces, Lecture Notes in Mathematics 394,Springer-Verlag, 1974.

15. Smith, B. D., Image reconstruction from cone-beam projections: Necessary and sufficient conditions and reconstruction methods, IEEE Trans. Med. Imaging, Vol. MI-4, No. 1, 1985, pp. 14-25.

16. Smith, B. D., Cone-beam tomography: recent advances and a tutorial review, Optical Engineering Journal, Vol. 29, May 1990, pp. 524-534.

Method	Parameter	$\varepsilon = 0.0$	$\varepsilon = 0.005$	$\varepsilon = 0.01$
I	$\alpha = 0.08$	0.0279	0.0294	0.0359
II	$\delta = 0.008$	0.0000	0.0048	0.0096
III	$\delta = 0.008$	0.0005	0.0137	0.0274
IV	$\gamma = 0.004$	0.0302	0.0315	0.0349

Table 1. Error Norms as functions of ε in Example 1 with N = 500

Method	Parameter	$\varepsilon = 0.0$	$\varepsilon = 0.005$	$\varepsilon = 0.01$
I	$\alpha = 0.08$	0.0275	0.0293	0.0365
II	$\delta = 0.008$	0.0001	0.0048	0.0096
III	$\delta = 0.008$	0.0005	0.0136	0.0273
IV	$\gamma = 0.001$	0.0174	0.0263	0.0431

Table 2. Error Norms as functions of ε in Example 2 with N = 500

Method	Parameter	$\varepsilon = 0.0$	$\varepsilon = 0.005$	$\varepsilon = 0.01$
I	$\alpha = 0.08$	0.0615	0.0618	0.0641
II	$\delta = 0.008$	0.0052	0.0052	0.0053
III	$\delta = 0.008$	0.0295	0.0330	0.0411
IV	$\gamma = 0.001$	0.0648	0.0678	0.0760

Table 3. Error Norms as functions of ε in Example 3 with N = 500

Third International Conference on Inverse Design Concepts and Optimization in Engineering Sciences (ICIDES-III), Editor: G.S. Dulikravich, Washington D.C., October 23-25, 1991.

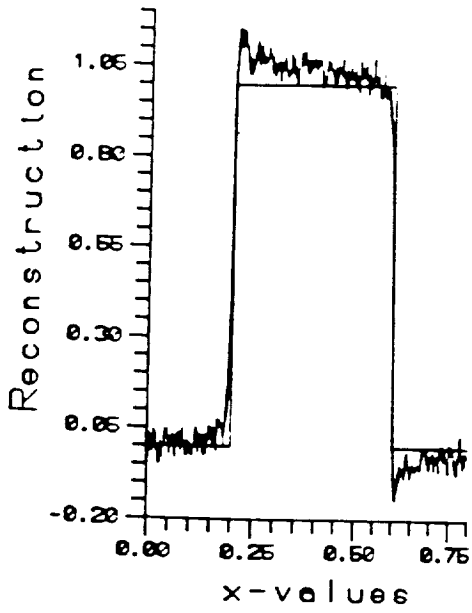

Fig. 1 Reconstruction with Method I
ε = 0.01, α = 0.08, N = 500

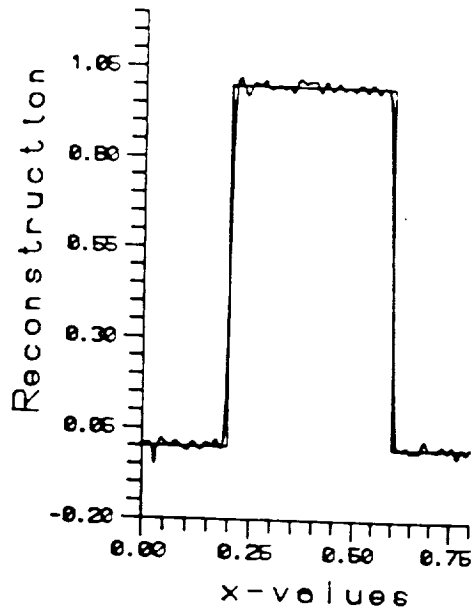

Fig. 2 Reconstruction with Method II
ε = 0.01, δ = 0.008, N = 500

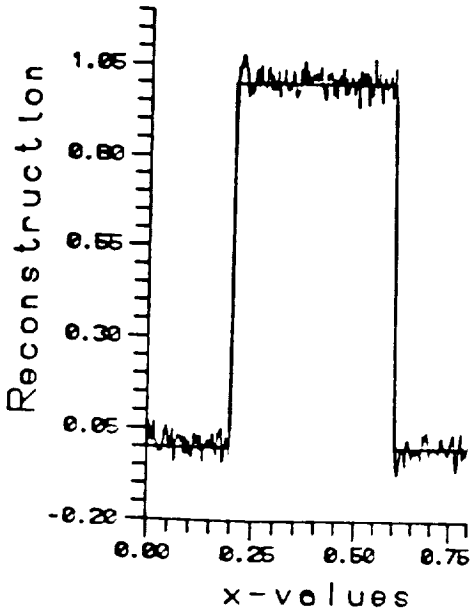

Fig. 3 Reconstruction with Method III
ε = 0.01, δ = 0.008, N = 500

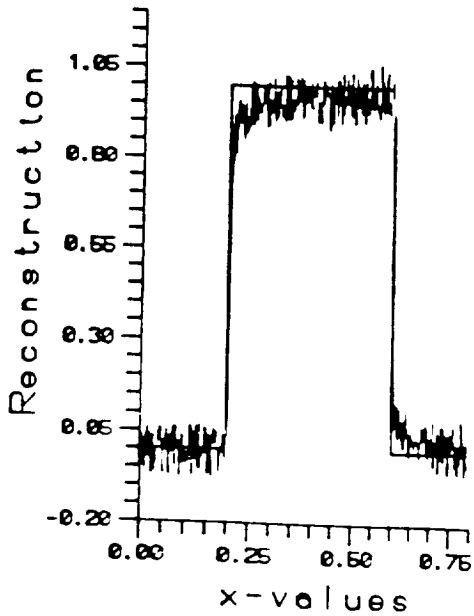

Fig. 4 Reconstruction with Method IV
ε = 0.001, γ = 0.001, N = 500